

# Oxygen effects on anisotropic photopolymerization in polymer matrices

Vadim V. Krongauz\* and E. Richard Schmelzer

*E. I. du Pont de Nemours and Company, Imaging Systems Research and Development,  
Experimental Station Laboratory, Box 80352, Wilmington, DE 19880-0352, USA*

*(Received 1 October 1990; revised 9 July 1991; accepted 31 July 1991)*

The influence of oxygen on polymerization kinetics in photopolymer films is studied using a fluorescence-based technique developed in this laboratory. Fluorescent *N*-vinylcarbazole monomer is used to monitor photopolymerization kinetics in the presence and absence of oxygen. Effects of oxygen at pressures up to 3 atm ( $3 \times 10^5$  Pa) on photopolymerization in various inert polymer matrices are studied. A reduction in the photopolymerization rate without induction period is observed in the presence of oxygen. A detailed computer analysis of the kinetics is presented. The unusual polymer spatial distribution is calculated and attributed to the anisotropy of illumination and the diffusion and reaction of the mobile oxygen and monomer species.

**(Keywords: photopolymer; film; photopolymerization; *N*-vinylcarbazole; fluorescence; polymer matrix; oxygen; kinetics; diffusion; anisotropy)**

## INTRODUCTION

The effects of oxygen on polymerization kinetics in solutions have been extensively studied<sup>1</sup>. Oxygen reacts with organic radicals forming peroxide radicals, thus decreasing the polymerization rate and altering the reaction path and chain-length distribution of the resulting polymer. However, oxygen effects on photopolymerization in highly viscous solutions under anisotropic reaction conditions produced by one-sided illumination of the samples have not been previously investigated. Inhibition and the induction periods due to the presence of oxygen have been widely reported in previous publications on photopolymerization. However, few reports exist concerning oxygen effects on photopolymerization in plasticized polymer matrices such as those used in imaging and electronics materials<sup>2</sup>.

Photopolymers are a class of photoimaging materials consisting of a plasticized polymer matrix in which a photoinitiator, monomer and a variety of other compounds are dissolved<sup>3</sup>. Photopolymers are used in printing, electronics and holography. Many peculiarities in the photopolymerization of such materials arise from the unidirectional illuminated and high viscosity of the solvent dissolved in the matrix. The illumination of one side of the high optical density film leads to a higher number of radicals formed closer to the illuminated surface and a larger consumption of reactive species near this surface. As monomer, oxygen and other reactive molecules are consumed, more of these species migrate towards the light from the interior of the film. Monomer and oxygen molecules diffuse in the plasticized matrix much faster than the forming polymer radicals. The result

is an anisotropic deposit of polymer in the matrix which we shall examine. In the particular case reported here the main contributor to the high optical density of the film is immobile initiator.

It is difficult to monitor the photopolymerization kinetics of such systems, and especially difficult to do real-time monitoring during photopolymerization. In solutions, oxygen effects on polymerization were often studied using luminescence quenching methods<sup>3,4</sup>. However, fluorescence and phosphorescence quenching techniques require the introduction of appropriate chromophores into the polymeric system, which can alter the property of the material studied. Another deficiency of the quenching methods is that only a limited range of diffusion rates can be measured because they must be compatible to the tracer fluorescence life times<sup>3,4</sup>.

We describe a recently developed, direct and non-destructive technique for monitoring photopolymerization kinetics and accompanying molecular transport<sup>5-7</sup>. The technique detects the change in intensity of the photopolymer film fluorescence due to migration of the fluorescent monomer towards the illuminated side of the film. The fluorescence is monitored at the isobestic point of the monomer and polymer emission spectra. Previously we were able to observe monomer transport accompanying photopolymerization<sup>5-7</sup>. An extensive mathematical model of the anisotropic photopolymerization in polymer films was developed and applied to the analysis of the obtained data<sup>7</sup>. We present here the extension of this work. In the present studies we investigate the effects of oxygen on the kinetics of photopolymerization in a plasticized polymer matrix. We attempt to circumvent the inability to monitor reactants redistribution through the film during photopolymerization, using a computer simulation in conjunction with the data on diffusion-controlled polymer formation.

\* To whom correspondence should be addressed

## EXPERIMENTAL

*Materials and reagents*

The photopolymer film used in this investigation consisted of poly(vinyl acetate) (PVA) (Monomer-Polymer and Dajac Laboratories, Inc.), inert polymeric matrix (binder), *o*-chloro-hexaphenylbiimidazol initiator, *N*-vinylcarbazole (NVC) monomer and plasticizers<sup>2,5</sup>. NVC was the only fluorescent polymerizable component (Monomer-Polymer and Dajac Laboratories, Inc.). Suprasil-1 quartz slides (Amersil Inc.) were used as the film support. The polymer solutions were coated on these slides with a coating knife, giving films around  $25 \pm 2 \mu\text{m}$  thick<sup>5-7</sup>. Oxygen, nitrogen and oxygen-nitrogen mixtures used in the experiments were supplied by Union Carbide Corporation, Linde Division. Poly(vinyl butyrate) (PVB) and cellulose acetate butyrate (CAB) (Monomer-Polymer and Dajac Laboratories, Inc.) were used in some experiments as alternative binders.

*Apparatus and procedures*

The experimental set-up is similar to that used in earlier experiments and is described in detail elsewhere<sup>5,6</sup>. However, the photopolymerization is conducted in a controlled atmosphere. To control the environment the sample is placed in a stainless steel vacuum chamber. A Varian Corporation stainless steel 38 mm six-way cross is used as the body of the vacuum chamber. The chamber is equipped with three sapphire windows to enable monitoring of light emission and absorption by the sample. A standard vacuum system with a mercury diffusion pump is used to evacuate the chamber. The sample is placed in a chamber using a rigid holder at a 45° angle relative to the direction of the excitation light beam. The photopolymer film is illuminated from the side which is in contact with the surrounding atmosphere. The fluorescence emitted by the sample is monitored from the opposite side of the film (*Figure 1*). The detection of

fluorescence is done at a 90° angle to the direction of excitation. A 51 mm head-on photomultiplier tube and a Stanford Research System photon counter and pre-amplifier, controlled by a personal computer, are used for the signal collection and processing<sup>5</sup>.

In all experiments 295 nm u.v. light is used for the illumination of the photopolymer samples, while the emission is monitored at 400 nm. The internal absorption of the fluorescence is negligible at this wavelength<sup>5,6</sup>. The exciting light is attenuated to prevent decomposition of NVC and poly(*N*-vinylcarbazole) (PVCA).

In a typical run a sample is placed in a vacuum chamber, the chamber is sealed and degassed at  $1.333 \times 10^{-5}$  Pa for approximately 30 min. Then the outlet valve is closed and oxygen, nitrogen or the mixture of oxygen and nitrogen is let into the chamber through the inlet valve at a pressure of approximately 2 atm ( $2 \times 10^5$  Pa). After degassing and pressurizing the sample, the time dependence of fluorescence is recorded.

*Principle of technique*

The method is based on monitoring the change in intensity of the fluorescence emitted by a plasticized polymer film containing the fluorescent monomer, NVC. The film used in the experiments had a high optical density due to absorption by non-polymerizing reactants such as sensitizer and initiator at the wavelength of the fluorescence excitation light (295 nm). The illumination of one side of the film with u.v. light leads to polymerization of the dispersed monomer and reduction of its concentration predominantly near the illuminated surface. Thus, during this photopolymerization reaction a concentration gradient of monomer develops and the monomer diffuses across the film towards the illuminated surface. Oligomers and the PVCA radicals that form, migrate out of the reaction zone very slowly or possibly not at all, due to their large size, so the polymer accumulates near the illuminated surface. Since only the monomer and resulting polymer are fluorescent, an increase in concentration of the polymer near the illuminated surface increases the total number of illuminated fluorescing carbazyl groups (major contribution to the high optical density came from unrelated species) and increases the fluorescence intensity (*Figure 2*). This increase in fluorescence intensity is used to monitor the photopolymerization kinetics at the isobestic point of the monomer and polymer spectra (400 nm). Under conditions of diffusion-controlled kinetics, and known photopolymer film thickness, the monomer diffusion coefficient is deduced<sup>5-7</sup>. The technique is applicable only to systems where oligomer radicals diffuse more slowly than monomer<sup>6</sup>. We observed no fluorescence quenching by oxygen. Plasticized films containing NVC or PVCA were degassed and placed in 3 atm ( $3 \times 10^5$  Pa) of N<sub>2</sub> or O<sub>2</sub>. In both cases we observed identical fluorescence intensity. Additional experiments were conducted by bringing the photopolymerization to completion in an oxygen-free environment, and then exposing it to oxygen. No change in the fluorescence intensity was detected in this case either. Since the fluorescence yield was independent of oxygen concentration the fluorescence-based technique described here was suitable for investigation of oxygen effects on photopolymerization in a particular set of formulations.

The absence of quenching of NVC and PVCA dissolved in a plasticized matrix can be rationalized

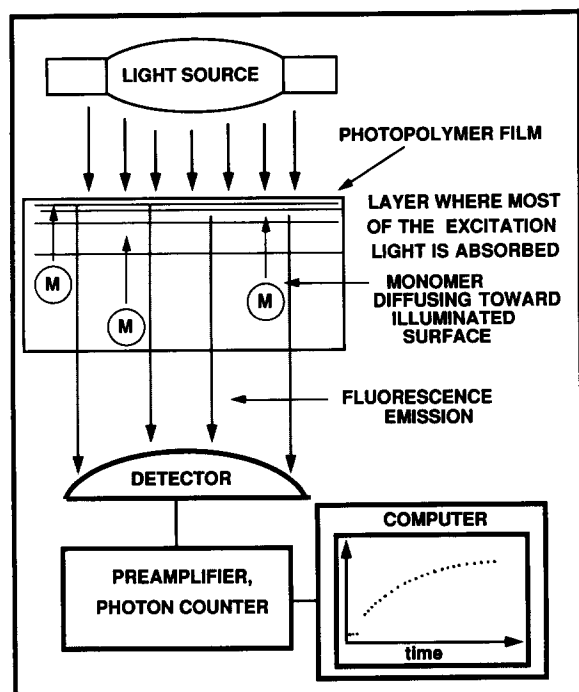


**Figure 1** Schematic diagram of the experimental set-up for the fluorescence detection measurements of photopolymerization kinetics in films

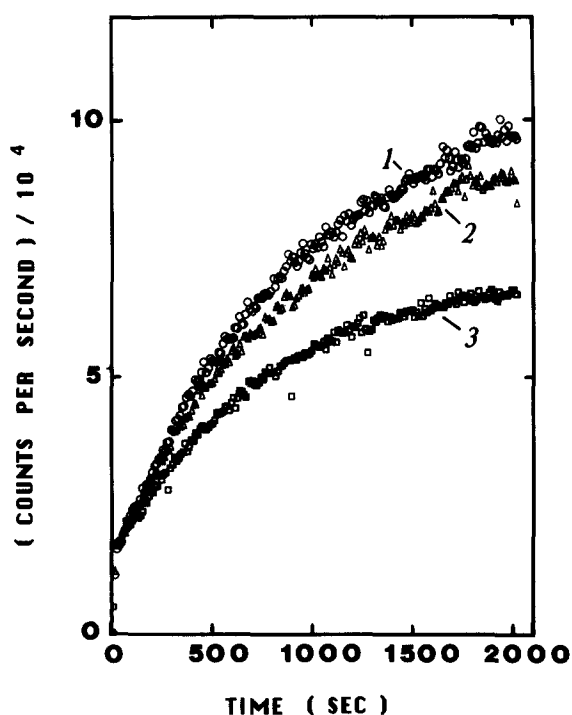


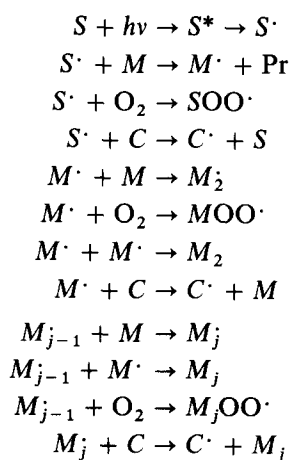
**Figure 2** Fluorescence detection kinetics of photopolymerization at various concentrations of oxygen in surrounding atmosphere: 1, neat nitrogen; 2, 0.05% oxygen in nitrogen; 3, 0.5% and higher concentration of oxygen in nitrogen

as follows. Oxygen is a dynamic quencher requiring collisional 'contact' with the excited molecule. In our matrix oxygen diffusion is slow ( $10^{-7} \text{ cm}^2 \text{ s}^{-1}$ ) and oxygen concentration in the matrix is low ( $<10^{-3} \text{ M}$ ) therefore the rate of quenching would be relatively low as well. The life time of NVC and PVCA fluorescence in polymer binders is less than 15 ns<sup>8,9</sup>. Thus, dynamic quenching by oxygen probably cannot compete with other deactivation processes, explaining the observed behaviour.

#### KINETIC MODEL AND COMPUTATIONS

To understand the role of oxygen on anisotropic polymerization in a film one has to take into account not only oxygen reactions with the radical species, but also diffusion of oxygen towards the illuminated surface from the bulk of the film due to oxygen consumption at the surface in these reactions.

A conventional free radical polymerization mechanism is adopted for the kinetic model<sup>1</sup>.



See Nomenclature for explanation of symbols. The rate of polymer diffusion in a polymer is low, therefore chain termination due to recombination of high molecular weight radicals is a relatively slow process and has been omitted from the kinetic scheme.

Restrictions are imposed on some of the steps because of the limited mobility of the larger species in the matrix. The concentration of monomer radicals is low and polymerization due to migration of the monomer radicals,  $M\cdot$  out of the illuminated region was omitted from consideration.

#### Kinetic equations

A detailed discussion of the approximations used in differential equations describing the kinetics of radical photopolymerization in the presence of molecular diffusion is given elsewhere<sup>7</sup>. In Table 1 a list of the equations used in calculations is presented.

Values for all the parameters are based on the experimental data obtained in this laboratory and from the literature. The set includes the thickness ( $24.5 \mu\text{m}$ ) and initial concentrations of monomer (8 wt%), chain transfer agent (2.3 wt%) and initiator (2 wt%) used in the experiments. An equilibrium oxygen level of 90 ppm ( $3 \times 10^{-6} \text{ mol cm}^{-3}$ ) is assumed typical of oxygen concentrations in viscous organic liquids and polymers exposed to air at room temperature<sup>10,11</sup>. The values of the oxygen diffusion coefficient evaluated in a similar polymer matrix<sup>10-12</sup> range from  $10^{-10}$  to  $10^{-7} \text{ cm}^2 \text{ s}^{-1}$ . In water at room temperature oxygen diffusivity was reported to be  $3 \times 10^{-5} \text{ cm}^2 \text{ s}^{-1}$  while in benzene cyclohexane and ethanol<sup>13</sup> the oxygen diffusivity was  $3 \times 10^{-4} \text{ cm}^2 \text{ s}^{-1}$ . We studied plasticized polymers for which no experimental data for oxygen diffusivity was reported, and therefore extrapolated the diffusivity of oxygen in our films from literature data<sup>10-13</sup>. The selected value of the oxygen diffusion coefficient was  $10^{-7} \text{ cm}^2 \text{ s}^{-1}$ . Rate constants of  $1.2 \times 10^{10} \text{ cm}^3 (\text{mol s})^{-1}$  for chain propagation and  $1.5 \times 10^{11} \text{ cm}^3 (\text{mol s})^{-1}$  for oxygen scavenging were employed based on similar values in the literature for a wide variety of polymerization systems<sup>14,15</sup>. The extinction coefficient<sup>16</sup> for the NVC and PVCA is  $3 \times 10^7 \text{ cm}^3 (\text{mol cm})^{-1}$  at 295 nm. Intensity of the excitation light was  $2.5 \times 10^{-8}$  einsteins. The monomer diffusion coefficient was deduced earlier<sup>5-7</sup> to be equal to  $6 \times 10^{-9} \text{ cm}^2 \text{ s}^{-1}$  for one of our photopolymer formulations, which agrees with that found by the fluorescence-based method for monomers of similar size<sup>17</sup>.

#### Initial and boundary conditions

Initially all the ingredients, including oxygen, are uniformly distributed. It is assumed that all ingredients except oxygen (in the case of no covers) are confined to the film and hence their gradients vanish at the surfaces, an essential condition in the absence of mass transfer at boundaries. The oxygen gradient vanishes at the surface in the presence of an impermeable barrier layer. Alternatively, the oxygen concentration is constant at its atmospheric equilibrium level. It is not possible to have both surfaces exposed to air with the very thin photopolymer films. A supporting layer is necessary on one side for mechanical integrity.

The incident light beam has a fixed intensity. Experimentally the sample can be illuminated from both sides

**Table 1** Kinetic equations describing anisotropic photopolymerization (see Nomenclature for explanation of symbols)

Parameter	Equation
Local light intensity	$\partial I/\partial z = -I \left\{ \epsilon_s[S] + \epsilon_m([M] + [P]) + \sum_k (\epsilon_k[Q]_k) \right\}$
Photoinitiation	$\partial[S]/\partial t = -\epsilon_s[S]I$ (Rate) <sub>initiation</sub> = $-2\{\partial[S]/\partial t\}$
Propagation	(Rate) <sub>propagation</sub> = $K_p[M] \left\{ \sum_{j=1}^{\infty} [r^*]_j \right\}$
Monomer concentration	$\partial[M]/\partial t = D_m \{ \partial^2[M]/\partial z^2 \} - K_p[M] \left\{ \sum_{j=1}^{\infty} [r^*]_j \right\}$
Polymer concentration (converted monomer)	$\partial[P]/\partial t = K_p[M] \left\{ \sum_{j=1}^{\infty} [r^*]_j \right\}$
Termination	(Rate) <sub>termination</sub> = $\{K_T[O_2] + K_{CT}[C]\} \left\{ \sum_{j=1}^{\infty} [r^*]_j \right\}$
Oxygen concentration	$\partial[O_2]/\partial t = D_{O_2} \partial^2[O_2]/\partial z^2 - K_T[O_2] \left\{ \sum_{j=1}^{\infty} [r^*]_j \right\}$
Radicals	$\partial R^*/\partial t = 2(\partial S/\partial t) - \{K_T[O_2] + K_{CT}[C]\} \left\{ \sum_{j=1}^{\infty} [r^*]_j \right\}$ $R^* = \sum_{j=1}^{\infty} [r^*]_j$
Chain transfer agent	$\partial[C]/\partial t = -D_{CT} \partial^2[C]/\partial z^2 - \{K_{CT}[C]\} \left\{ \sum_{j=1}^{\infty} [r^*]_j \right\}$
Fluorescence intensity (observable)	$\partial(I)_{\text{fluorescence}}/\partial z = Iq\epsilon_m([M] + [P])$

by flipping the film. Incidence of the light beam in the model can be step-turned by 180° at a prescribed time for imaging on the 'flip-side'.

### Calculations

The geometry of the problem lends itself to a finite difference approach in the simultaneous solution of the partial differential equations by the method of points. The thickness of the film is divided on a set of non-uniform finite elements with the smallest elements near the surface in the vicinity of anticipated abrupt and rapid changes. Partial derivatives in the geometric variable,  $z$ , are approximated by three-point formulas with unequal intervals. The number of divisions in discretization is optional but computed results show 25 divisions give good accuracy at reasonable computing times. More points may be needed under extreme conditions; such a need becomes self-evident in examination of the results. The division into infinite elements between surfaces is symmetric about the midplane for ease in processing flip-side exposures.

Time derivatives of all the dependent-variables are integrated by a stiff differential equation solver (Gear algorithm<sup>18</sup>). Elements in the Jacobian are evaluated by numerical differencing. Results are recorded at selected fractional times of the overall exposure period.

## RESULTS AND DISCUSSION

### Oxygen concentration effects

In the presence of oxygen we observe the expected drop in the rate of the photopolymerization by monitoring a reduction in the fluorescence of the photopolymer film (Figure 2). Increasing the oxygen content in the atmosphere surrounding the degassed photopolymer leads to

a decrease of the radical concentration. This in turn results in slower growth of fluorescence intensity during photopolymerization. We did not observe any change in kinetics at oxygen concentrations in nitrogen atmosphere surrounding the illuminated film exceeding 0.5%. However, the rate of polymerization drops further when the reaction is run at 3 atm ( $3 \times 10^5$  Pa) of pure oxygen, indicating that we are indeed dealing with the effects produced when oxygen is absorbed by the photopolymer. Since oxygen concentration is low, and oxygen diffusion is slow in a polymer matrix, chain propagation successfully competes with the termination reaction and there is no noticeable induction period. The possible absence of an induction period in photopolymerization in a viscous medium is often overlooked since most of the literature is dedicated to polymerization in a liquid batch in which the oxygen diffusion coefficient is much higher than that of monomer<sup>1,15</sup>.

Model computations result in qualitatively similar kinetics (Figure 3) to that observed experimentally. There is no induction period in modelled anisotropic photopolymerization in the films in contact with oxygen. Naturally, the polymer yield decreases as the oxygen concentration in the film increases. Our computations indicate that for the existence of the induction period associated with oxygen, the difference between oxygen and monomer rates of reaction with radicals has to be much higher than those of the model system presented above. The DuPont holographic photopolymer film used as a basis for computations and in the experiments described above is designed to have low sensitivity to oxygen and short imaging time.

We intentionally avoid deducing the diffusion coefficients for oxygen and monomer using our model since some variables are not measured by us, but taken from the literature. Our experiments serve to verify the overall

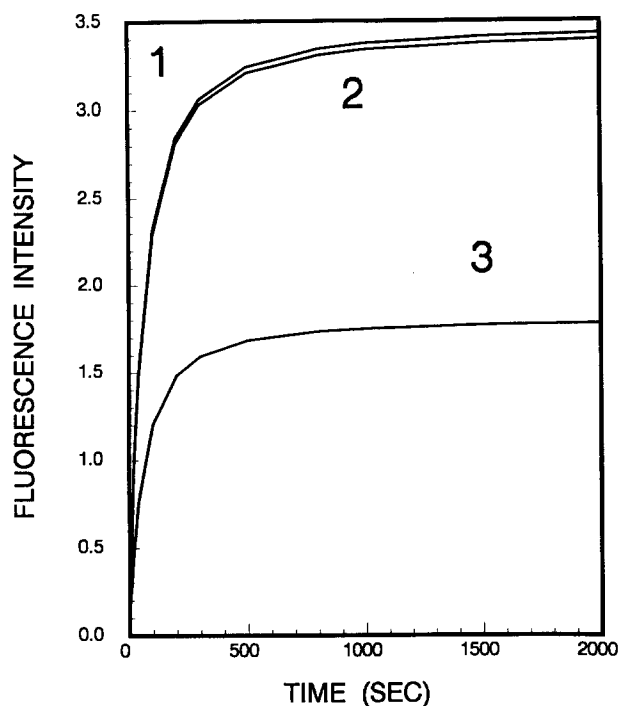


**Figure 3** Computed fluorescence detection kinetics of photopolymerization at various concentrations of oxygen in surrounding atmosphere: 1, neat nitrogen; 2, 0.05% oxygen in nitrogen; 3, 0.5% oxygen in nitrogen

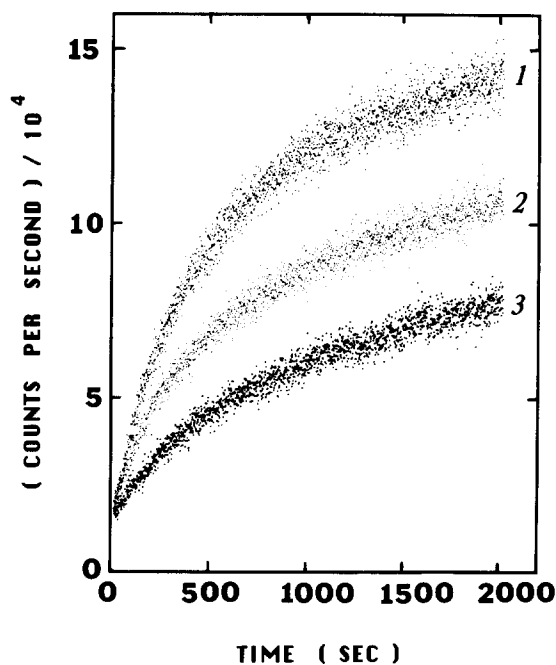


**Figure 4** Matrix dependence of photopolymerization kinetics in the absence of oxygen. The samples are degassed prior to conducting the experiment in nitrogen environment. Kinetics measured in: 1, cellulose acetate butyrate; 2, poly(vinyl butyrate); 3, poly(vinyl acetate)

qualitative validity of the model, while the model in turn is used to analyse the effects, such as polymer distribution across the film, which have not been measured experimentally so far.

#### Oxygen and matrix effects

We varied the polymer matrix (binder) used in the photopolymer formulation to change the diffusion coefficient of monomer and oxygen. CAB, PVB and PVA

were used. The photopolymerization kinetics were first recorded in a nitrogen atmosphere after degassing the film to ensure the absence of oxygen (Figure 4). These results were reported previously<sup>6</sup>. In that paper we treated the data using another simpler model<sup>6</sup> which did not consider diffusion of other components. The diffusion-controlled monomer polymerization in a narrow region near the illuminated surface was treated in this model as a surface evaporation, allowing the rate of monomer loss to be computed in terms of its diffusivity. The comparison of the experimental and computed curves is presented in Figure 5. The results show that monomer diffusion is faster in the CAB binder (Figure 5). It is reasonable to assume that oxygen diffuses faster in this binder as well. Faster oxygen diffusion results in a faster rate of formation of peroxide radicals and less PVCA formed. The data (Figure 6) demonstrate that in the presence of oxygen a larger drop in the polymerization rate occurs in the binder where the rate of monomer and oxygen diffusion is higher. In the presence of oxygen the rate of polymerization in CAB becomes lower than that in PVB and the highest rate of polymerization is observed in the PVA matrix. Apparently, the rate of oxygen diffusion is higher in CAB than in PVB and PVA. Therefore, oxygen competes with monomer and the chain transfer agent for the reaction with radicals more effectively in CAB than in PVA, thus slowing polymerization more in CAB than in PVA. Computations done using the more complete model support our explanation of the observed unequal drop in photopolymerization yields.

Since many parameters in our comprehensive model are not measured by us, we did not use this model for diffusion coefficient deduction. We used the data obtained by other techniques to show qualitative consistency of the observed data and data computed by our comprehensive model. In discussion of oxygen effects in different

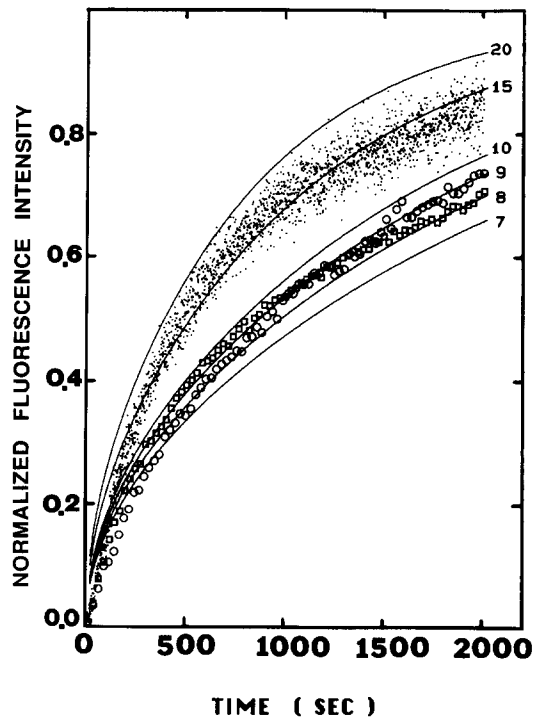


**Figure 5** Illustration of the monomer diffusion coefficient computations using the surface evaporation model. The numbers on the curves represent the values of diffusion coefficients used in computations of the curve ( $\times 10^{10}$ ). Kinetics measured in: cellulose acetate butyrate; poly(vinyl butyrate); poly(vinyl acetate)

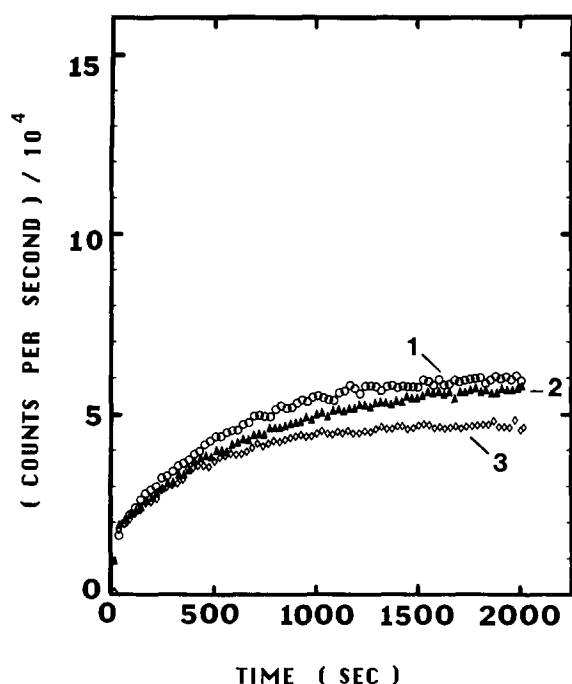


Figure 6 Kinetics of photopolymerization in different matrices in the presence of oxygen in: 1, poly(vinyl butyrate); 2, poly(vinyl acetate); 3, cellulose acetate butyrate

polymer matrices (binders) we took hypothetical binders with similar difference in diffusivities and modelled polymerization in these binders. The diffusion coefficient is proportional to the square of the diameter of the pore in the polymer matrix through which the molecule diffuses<sup>19</sup>. Therefore, in the first approximation we can assume that the ratio of oxygen diffusion coefficients in various matrices is equal to that of the monomer diffusion coefficients. Using the data of Figure 5 we find the ratio of monomer diffusion coefficients in CAB and PVA. Using our simpler model<sup>6</sup> we found that the monomer diffusion in CAB, occurs with  $D_{\text{MONOMER}} = 1.5 \times 10^{-9} \text{ cm}^2 \text{ s}^{-1}$ , while in PVA monomer diffuses with  $D_{\text{MONOMER}} = 0.9 \times 10^{-9} \text{ cm}^2 \text{ s}^{-1}$ . The ratio of these diffusion coefficients is 1.67. The oxygen diffusion coefficient correspondingly would change from  $10^{-7} \text{ cm}^2 \text{ s}^{-1}$  selected for previous calculations to  $6 \times 10^{-8} \text{ cm}^2 \text{ s}^{-1}$ . Substituting the new oxygen and monomer diffusion coefficients into the kinetic equations presented above, we computed the expected change in fluorescence intensity of the photopolymer film during exposure (Figure 7). The computations demonstrate that in the presence of oxygen, the rate of polymerization and the amount of polymer formed decrease more in the case of a matrix with a larger pore size, where diffusivity of small molecules is higher. Thus, computations qualitatively reproduce the experimental data of Figure 6 and confirm the explanation of the observed behaviour.

The model computations described above qualitatively reproduce the photopolymerization kinetics detected by fluorescence in the cases studied. It also provides an explanation for the unusually strong drop in polymerization rate in the presence of oxygen in a matrix where diffusivities are higher. Therefore, we may conclude that the model represents reasonably well the mechanism of the photopolymerization in the described photopolymer system. Moreover, we may employ the developed kinetic model to analyse those properties of the photopolymer film which cannot be easily detected experimentally. The

spatial distribution of the polymer forming in the film during film exposure to u.v. light is an example of such a property that is difficult to measure. Indeed, it is hard to devise a method for the analysis of the product distribution across a film 25  $\mu\text{m}$  thick. However, computer modelling can indicate the possible behaviour of the system. There are various problems with spatial non-uniformity and low rate of photopolymer imaging reported in the industrial literature<sup>18</sup> and ascribed to oxygen effects. We will examine these effects using our kinetic model.

#### Oxygen and anisotropic photopolymerization

Observation of non-uniform photopolymerization was previously reported by us<sup>7</sup>. When photopolymerization occurs in a film containing some oxygen acquired during the coating, but protected from the influx of oxygen by two cover sheets, the computed polymer yield distribution in the film was inhomogeneous<sup>7</sup> (Figure 8). There are several factors contributing to this inhomogeneity. The monomer consumption is higher near the illuminated surface where the light intensity is higher (Figure 9). However, larger amounts of radicals near the surface do not result in a higher polymer yield at longer times. This is because there is initially a greater concentration of oxygen in the film (Figure 10), and the radicals formed early on near the film surface are partially spent on oxygen removal. Mobilities of initiator and oligomer radicals are neglected in the model relative to the mobility of the monomer, oxygen and chain-transfer agent. Therefore, the loss of radicals due to reactions with oxygen is not compensated by diffusion. So the radical distribution and, consequently, polymer formation depend

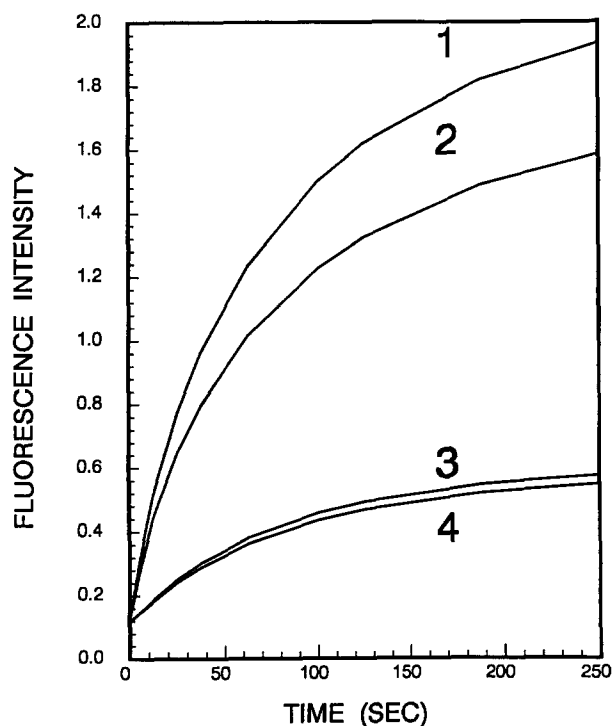


Figure 7 Computed kinetics of photopolymerization in different matrices: 1, high permeability matrix ( $D_{\text{MONOMER}} = 1.5 \times 10^{-9} \text{ cm}^2 \text{ s}^{-1}$ , no oxygen); 2, low permeability matrix ( $D_{\text{MONOMER}} = 0.9 \times 10^{-9} \text{ cm}^2 \text{ s}^{-1}$ , no oxygen); 3, high permeability matrix with 90 ppm of oxygen present ( $D_{\text{MONOMER}} = 1.5 \times 10^{-9} \text{ cm}^2 \text{ s}^{-1}$ ,  $D_{\text{OXYGEN}} = 1 \times 10^{-7} \text{ cm}^2 \text{ s}^{-1}$ ); 4, low permeability matrix with 90 ppm of oxygen present ( $D_{\text{MONOMER}} = 0.9 \times 10^{-9} \text{ cm}^2 \text{ s}^{-1}$ ,  $D_{\text{OXYGEN}} = 0.6 \times 10^{-7} \text{ cm}^2 \text{ s}^{-1}$ )

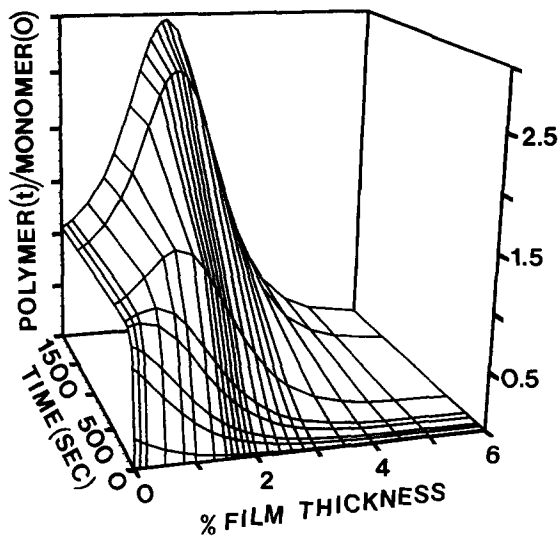


Figure 8 Dependence of the concentration of the forming polymer on distance from the illuminated surface at various times from the start of illumination. Both sides of the film are protected from contact with atmosphere

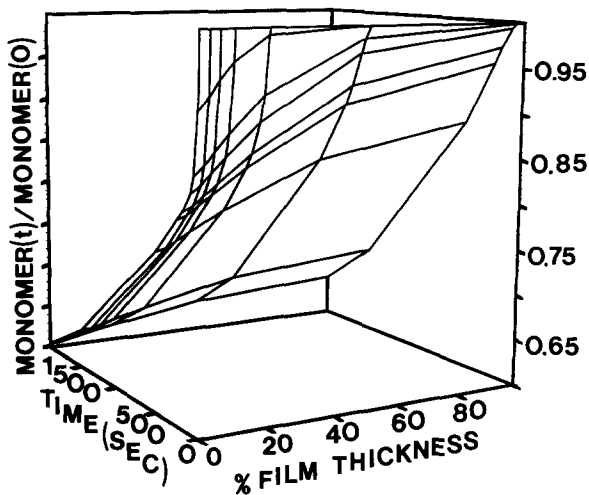


Figure 9 Monomer concentration as a function of distance from the illuminated surface and time of exposure. Both sides of the film are protected from contact with oxygen

When the exposed surface of a film is open to oxygen, the oxygen lost in the photochemical reaction is replenished by diffusion from the surrounding atmosphere during imaging. Considering the relatively high rates of oxygen diffusion, radicals near the illuminated surface, and deeper inside, are exposed to roughly constant oxygen concentrations. The model computations confirm this. Therefore, the resulting distribution of photopolymer is more uniform. As deeper layers of the film polymerize, the maximum polymer concentration reached through the film is constant (Figure 11). Of course, the maximum yield of polymer is lower than that for a protected film. This uniformity of image in the presence of oxygen is in great contrast to the intuitive picture of oxygen effect on image. It is generally believed that oxygen causes non-uniform photopolymerization in every instance. However, the results of our calculations demonstrate that in some cases the effect of oxygen on image formation in photopolymers is opposite to this, improving the uniformity. The calculated results of Figure 11 can be

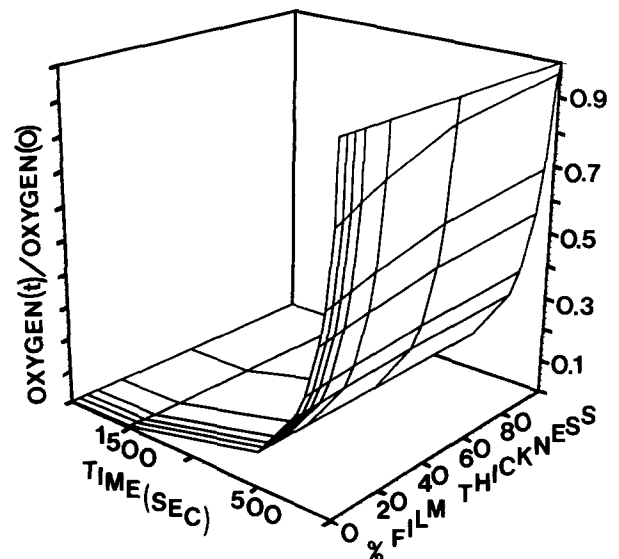


Figure 10 Dependence of oxygen concentration on distance from the illuminated surface at different times from the start of illumination. Both sides of the film are assumed to be covered by an oxygen impermeable polymer

strongly on the region and rates of oxygen and monomer diffusion. Since the oxygen diffusion rate is higher than that of monomer, oxygen concentration throughout the film declines relatively fast (Figure 10) while plenty of the monomer still remains deeper within the film (Figure 9). Thus, the radicals produced deeper within the polymer film survive longer. Because of reduced oxygen termination of the chains, longer polymer molecules can be produced, and conversion of monomer becomes higher some distance away from the illuminated surface. The result is non-uniformity of the polymer distribution and corresponding image (Figure 8). This non-uniformity is particularly troublesome in the case of systems where imaged and unimaged (non-polymerized) regions are differentiated by dissolving or peel-apart methods<sup>2</sup>.

Various techniques of reduction of image non-uniformity are used in printing. We believe that image distortion can be reduced not only by conducting photopolymerization in an oxygen-free environment, but also by exposing the films while keeping the oxygen concentration constant.

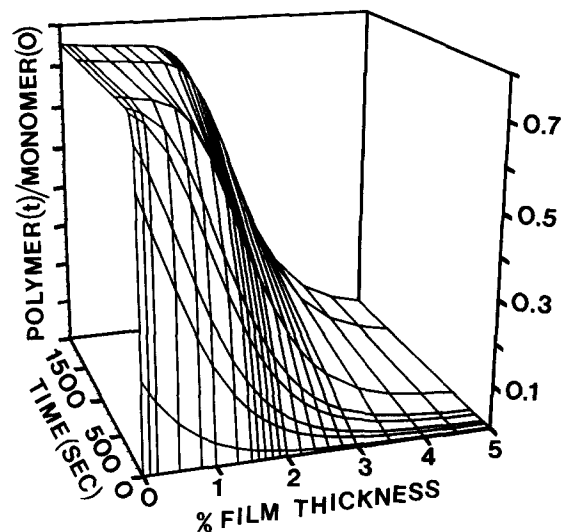
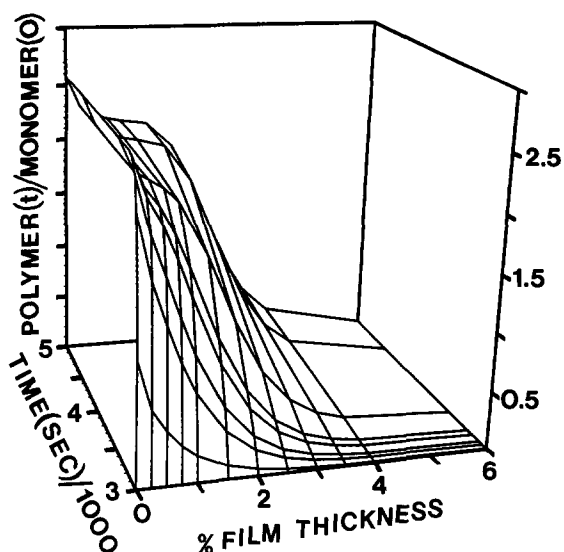


Figure 11 Polymer distribution in film at various times from the start of illumination. The illustrated surface is in contact with oxygen



**Figure 12** Polymer distribution through the film thickness at different times. This distribution has resulted from exposure started immediately after the reverse side of the film was exposed to light for 3000 s. Both sides of the film were protected from contact with oxygen

applied in practice. In applications where great depth of polymerization is required, such as photoresists and flexographic plates<sup>2,20</sup>, the uniformity of imaging can be improved by changing the oxygen exposure of the film in addition to the traditional variation of light wavelength and intensity.

#### Two-sided exposure

As mentioned above, in many industrial applications of photopolymers, oxygen effects present a problem, reducing the photospeed of the materials and distorting the shape of resulting pixels<sup>21</sup>. A variety of techniques are used to reduce the problems associated with oxygen inhibition of photopolymerization. In the case of film with a high optical density isolated from air by cover sheets, oxygen concentration in the photopolymer film can be lowered by pre-exposing the film to light (u.v. in the present case) from one side and only then using the flip-side of the film for the desired image. Indeed, computations indicate a drastic decrease in oxygen contents in the isolated film even after a relatively short exposure. The decrease in oxygen content after one-sided exposure of the film is presented in *Figure 10*. At low exposure times oxygen concentration is reduced faster near the illuminated surface, and later when oxygen has the time to diffuse the concentration becomes uniformly low throughout the film thickness. The exposure of the reverse side of the photopolymer film results in higher polymer yield and image uniformity (*Figure 12*). The yield of the polymer near the surface of the photopolymer film, protected on both sides, is more than double that resulting from the first exposure. A more uniform depth distribution of the polymer results upon the reverse side exposure. Results of computations (*Figure 12*) illustrate and validate the benefits of the empirical method of oxygen removal by pre-exposure.

Naturally, the best defence against reduced photopolymerization yield and severe imaging non-uniformity is removal of oxygen in the films. However, under most industrial conditions degassing is rather impractical and often impossible, therefore pre-exposure from the

reverse side is a good alternative technique for eliminating oxygen.

#### CONCLUSIONS

Oxygen effects on the kinetics of radical photopolymerization in photopolymer films were experimentally observed and modelled. To the best of our knowledge, this is the first time this has been done in an anisotropic system in a viscous medium. It is clear from the data presented that oxygen effects on radical polymerization in a matrix are not as simple as commonly thought. Complexity results mainly from the anisotropy of the imaging and the absence of mixing. Under such conditions, long range molecular migration becomes a determining factor in the competition between monomer and oxygen for reaction with the initiator radicals and growing polymer chains. In solid or highly viscous systems, where the rates of diffusion-controlled oxygen and monomer reactions with radicals are comparable, an induction period attributed to oxygen may not be observed in a closed system.

The removal of oxygen from photopolymers prior to imaging leads to a higher polymerization rate and a more uniform polymer distribution. In practice, degassing the film is complicated so alternative measures, such as pre-exposure from the reverse side or the exposure of the imaged side of the photopolymer film to oxygen, can be beneficial.

The model and experimental data presented here provide a reasonable illustration of the type of phenomena one has to consider when dealing with photopolymerization in the presence of oxygen.

#### ACKNOWLEDGEMENTS

We would like to acknowledge Mr Robert Yohannan for his assistance in conducting some of the experiments. We would also like to thank Dr Andrew Weber for sharing with us different polymer binders, and Mr Mikhail Grinberg for help with the graphics preparation for the manuscript.

#### REFERENCES

- 1 Bagdasarian, Kh. S. 'Theory of Free-Radical Polymerization', Israel Program for Scientific Translations, Jerusalem, 1968, IPST Cat. No. 2197
- 2 Cohen, A. B. and Walker, P. in 'Imaging Processes and Materials' (Ed. J. M. Strurge), Neblette's 8th Edn, Van Nostrand Reinhold, New York, 1989
- 3 Smith, B. A. in 'Photophysical and Photochemical Tools in Polymer Science' (Ed. M. A. Winnik), NATO ASI Series C: Mathematical and Physical Sciences, D. Reidel Publishing, The Netherlands, 1986, Vol. 182, pp. 397-407
- 4 Guillet, J. E. in 'Photophysical and Photochemical Tools in Polymer Science' (Ed. M. A. Winnik), NATO ASI Series C: Mathematical and Physical Sciences, D. Reidel Publishing, The Netherlands, 1986, Vol. 182, pp. 467-494
- 5 Krongauz, V. V. and Yohannan, R. M. *Polymer* 1990, **31**, 1130
- 6 Krongauz, V. V. and Yohannan, R. M. SPIE OE/Lase Conference Proceedings, Los Angeles, 1990, Vol. 1213, pp. 174-183
- 7 Krongauz, V. V., Schmelzer, E. R. and Yohannan, R. M. *Polymer* 1991, **32**, 1654
- 8 Kitamura, N., Inoue, T. and Tazuke, S. *Chem. Phys. Lett.* 1982, **89**(4), 329
- 9 Ito, S., Takami, K., Tsujii, Y. and Yamamoto, M. *Macromolecules* 1990, **23**, 2666
- 10 Moisan, J. Y. in 'Polymer Permeability' (Ed. J. Comyn), Elsevier, London, 1988, p. 127



- 11 Chu, D. Y., Thomas, J. K. and Kuczynski, J. *Macromolecules* 1988, **21**, 2094
- 12 Timpe, H. J., Basse, B., Muller, F. W. and Muller, C. *Eur. Polym. J.* 1987, **23**(12), 967
- 13 Krieger, I. M., Mulholland, G. W. and Dickey, C. S. *J. Phys. Chem.* 1967, **71**(4), 1123
- 14 Walling, C. 'Free Radicals in Solution', John Wiley, New York, 1957
- 15 Pryor, W. A. 'Free Radicals', McGraw-Hill, New York, 1966
- 16 Ellinger, L. P. *Polymer* 1964, **5**(1), 559
- 17 Billingham, N. C., Calvert, P. D. and Uzuner, A. *Polymer* 1990, **31**, 258
- 18 Gear, C. W. in 'Information Processing 68' (Ed. A. J. H. Morrell), North Holland, Amsterdam, 1969, pp. 187-193; *Comm. ACM* 1971, **14**, 176
- 19 Hirschfelder, J. O., Curtiss, C. F. and Bird, R. B. 'Molecular Theory of Gases and Liquids', J. Wiley, New York, 1954
- 20 Omote, T., Yamaoka, T. and Koseki, K. *J. Appl. Polym. Sci.* 1989, **38**, 389
- 21 Kuchta, A. D. *Electronic Manuf.* 1988, **34**, 8

#### NOMENCLATURE

$C$	Chain transfer agent
$D_L$	Diffusion coefficient of component L ( $\text{cm}^2 \text{s}^{-1}$ )
$f$	Parameter to account for presence of fluorescence quenchers in photopolymer formulations

$I$	Light intensity
$K_L$	Rate constant for component L
$M$	Monomer
$M_j$	Radical containing $j$ monomeric units
$P$	Polymer
$q$	Average quantum yield
$[Q]_k$	Concentration of $k$ th component of photopolymer
$[r^*]_j$	Concentration of radical of chain length $j$
$R$	Radical
$S$	Photoinitiator
$t$	Time
$z$	Normal distance below film surface
$\epsilon_L$	Extinction coefficient for component L
$\epsilon_m$	Average extinction coefficient of carbazyl groups in monomer and polymer

#### Subscripts

CT	Chain transfer
$k$	$k$ th component of photopolymer formulation
$m$	Monomer
$p$	Propagation
$s$	Initiator
$T$	Termination